

Transition from placental to air breathing stimulates haem-oxygenase-1 expression without functional consequence for pulmonary vascular adaptation in pigs and mice

^{1,2}Salome J. Stanford, ²Alison A. Hislop, ¹Ute Oltmanns, ³Elizabeth G. Nabel, ³Hong Sang, ²Shelia G. Haworth & ^{*1}Jane A. Mitchell

¹Cardiothoracic Pharmacology, UCCM, The Royal Brompton & Harefield N.H.S. Trust, Imperial College, National Heart and Lung Institute, Dovehouse Street, Sydney Street, London, SW3 9LY; ²Developmental Vascular Biology and Pharmacology, Institute of Child Health, 30 Guilford Street, London WC1N 1EH and ³Vascular Biology Branch, National Heart, Lung, and Blood Institute, Bethesda, Maryland, MD 20892, U.S.A.

1 In systemic vessels, haem-oxygenase (HO) is induced during oxidative stress and known to modulate vasodilatation and vascular remodelling. At birth, with the transition from placental to air breathing, the pulmonary vessels are exposed to oxidative stress and undergo well-documented remodelling processes. Thus, we investigated the role of HO in the lung during adaptation to extra-uterine life using a pig and mouse model. In addition to the novel data presented with regard to one isoform, HO-1, this study is among the first to describe the pulmonary vascular remodelling in the mouse after birth.

2 We show, for the first time, that another isoform, HO-2, is present constitutively at birth and HO-1 protein is induced in the porcine and murine lung after birth in vascular and airway structures, peaking at 14 days in the pig and at about 4 days in the mouse. Furthermore, we show that HO-1 mRNA declines after birth in the mouse lung.

3 Inhibitors of HO did not modify vasodilator responses in vessels from 14-day-old pigs.

4 Moreover, lungs from HO-1-deficient mice developed normally after birth.

5 HO-1 is induced at birth but plays no role in the development of vasodilator responses or remodelling that occurs at this time. These data suggest that HO-1 expression at birth is a redundant response to oxidative stress in the lungs of healthy mammals. However, it remains possible that this pathway protects if complications occur during or after birth.

British Journal of Pharmacology (2005) **144**, 467–476. doi:10.1038/sj.bjp.0705988

Published online 17 January 2005

Keywords: Vascular remodelling; haem-oxygenase; cGMP; development; vasodilation

Abbreviations: ACh, acetylcholine; CO, carbon monoxide; CrMP, chromium mesoporphyrin; *Hmox*, HO-1 knock out; HO, haem-oxygenase; HRP, horseradish peroxidase; Hsp-32, heat shock protein 32; L-NAME, *N* ω -Nitro-L-arginine methyl ester; LV + S, left ventricle plus septum; NB, newborn; NO, nitric oxide; NOS, NO synthase; OD, optical density; PBS, phosphate buffered saline; PCR, polymerase chain reaction; PPHN, persistent pulmonary hypertension of the newborn; ROS, reactive oxygen species; RV, right ventricle; sGC, soluble guanylyl cyclase; SNP, sodium nitroprusside; SnPP, tin protoporphyrin

Introduction

Haem-oxygenase (HO; EC 1.14.99.3) is the first enzyme in the conversion of haem to carbon monoxide (CO), free iron and biliverdin. Biliverdin is rapidly converted by a second enzyme, biliverdin reductase, to bilirubin. Two major isoforms of HO, HO-1 and HO-2, have now been identified and cloned. A third form, HO-3, has been cloned in the rat (McCoubrey *et al.*, 1997). HO-2 is the 36 kDa, constitutive form of the enzyme. It is expressed at high levels in the testes and brain (Ewing & Maines, 1995) and has also been localised to the vascular endothelium (Zakhary *et al.*, 1996). By contrast, HO-1 (Hsp-32) is a 32 kDa enzyme, highly inducible in many cell types in response to a wide range of inflammatory mediators and, most notably, by reactive oxygen species (ROS) and oxidative stress.

HO-1 is always present in the spleen where activity is maintained as a result of constant exposure to the haemoglobin released during the breakdown of aging erythrocytes (Braggins *et al.*, 1986).

The products of HO are increasingly recognised as important modulators of vascular form and function in the systemic circulation. In the case of CO, parallels have been drawn between its actions and those of the ubiquitous vasodilator gas, nitric oxide (NO). The vasodilator actions of both NO and CO are thought to be mediated by the activation of soluble guanylyl cyclase (sGC) (Morita *et al.*, 1995) and both can influence vascular remodelling. In rat thoracic aortic smooth muscle cells, CO derived from HO-1 is an autocrine inhibitor of cell growth (Peyton *et al.*, 2002). Recognition of these properties of CO has led to suggestions that CO gas, or molecules that release CO (Mottlerini *et al.*, 2002),

*Author for correspondence; E-mail: j.a.mitchell@ic.ac.uk
Published online 17 January 2005

may represent new therapies to treat different forms of cardiovascular disease in much the same way as NO and nitro vasodilators are used currently. Bilirubin and biliverdin are well-documented antioxidants, the release of which might protect the vasculature from oxidative stress and injury (Hayashi *et al.*, 1999; Durante, 2002).

HO-1 may also be an important protective enzyme system in the pulmonary circulation. HO-1 is induced in animal models of adult pulmonary hypertension (Minamino *et al.*, 2001; Carraway *et al.*, 2002) and HO-1 transgenic mice are protected from hypoxia-induced pulmonary inflammation, hypertension and vessel wall hypertrophy (Minamino *et al.*, 2001). However, little is known regarding the role of HO in the foetal and newborn (NB) pulmonary circulation.

Blood flow is low in the pulmonary circulation of the foetus as a result of the high pulmonary vascular resistance that occurs not only as a result of vessel architecture, but also due to low oxygen tension and the release of vasoactive mediators. Pulmonary vascular resistance falls rapidly after birth as the pulmonary vasculature adapts to extra-uterine life. The regulation of pulmonary vascular resistance during this transition period is complex and not fully understood. Animal studies indicate rapid remodelling of the vascular endothelial and smooth muscle cells. Specifically, a reduction in the overlap of adjacent smooth muscle cells, together with a flattening of the lining endothelial cells, occurs such that an immediate decrease in vessel wall thickness, and increase in lumen diameter, is observed (Haworth & Hislop, 1981). Pharmacological studies describe maturation changes of vasoactive pathways in the endothelium of arteries and veins (Liu *et al.*, 1992; Tulloh *et al.*, 1997; Arrigoni *et al.*, 1999) during this time.

In the neonatal period, with the change from placental to air breathing, the lungs will experience oxygen for the first time. The dramatic change from no oxygen to oxygen is similar to the processes of re-oxygenation after ischemia, a recognised stimulus for HO induction in other organs (Bak *et al.*, 2003). Thus, HO-1 may play a role in the regulation of pulmonary vascular resistance at birth. Such features are important to understand because in a small proportion of NB babies such adaptive processes fail, and persistent pulmonary hypertension of the NB (PPHN) may occur.

The aims of the current study were therefore to address (i) how HO levels may change with the first breath at birth and (ii) investigate how changes in HO expression may impact on the normal adaptive changes that occur in the lung in the first few hours and days after birth. We have employed classical organ bath protocols using inhibitors of HO activity in blood vessels from young pigs where HO-1 was found to be relatively high. In addition, we have studied the lungs of HO-1-deficient mice (Duckers *et al.*, 2001) just after birth in order to determine the effects of induction of remodelling of pulmonary structures that typify adaptation at this time.

Methods

Porcine studies

Large White pigs supplied by the Royal Veterinary School (Camden, London) were used for this study. Lungs were harvested from foetal piglets, NB animals (<5 min), 1-, 3- and

14-day-old piglets and adult animals. The young piglets were killed with an overdose of sodium pentobarbitone (100 mg kg⁻¹). Tissue from adult pigs was obtained from a local abattoir. For use in Western blotting, whole lung tissue from piglets, or sections of airway and intrapulmonary artery dissected out from the lower lobes, were snap frozen within 60 min of death. Lung tissue from adult animals was transported to the laboratory on ice-cold Krebs–Henseleit solution and snap frozen within 2 h. For immunohistochemistry, lung tissue was fixed overnight in 10% formol saline, before being transferred into 70% alcohol and embedded in paraffin wax. For organ bath studies conduit intrapulmonary arteries were dissected out from the lower lobes of lungs taken from 14-day-old piglets, vessels were placed immediately into the organ bath.

Murine studies

Lungs were harvested from 1-, 4-, 10-, 14-day-old and adult mice (C57BL/6J). Juvenile mice were killed by decapitation, adult animals by a lethal dose of sodium pentobarbitone (60 mg kg⁻¹). Whole lung tissue was snap frozen immediately on death and used for Western blotting. For immunohistochemistry, lungs from 1-, 3–5-, 14-day-old and age-matched adult HO-1 knockout (*Hmox1*^{-/-} mice (C57BL/6J cross background) (Duckers *et al.*, 2001) or *Hmox1*^{+/+} (C57BL/6J) mice were collected and prepared in the laboratory of Dr E.G. Nabel as follows: lungs were inflated *via* the trachea with 10% formol saline (under 20 cm of pressure) before being removed from the chest cavity with the heart still attached. Lung tissue was fixed overnight in 10% formol saline and then transferred to 70% alcohol for storage and shipment prior to being embedded in paraffin wax for immunohistochemical studies. For adult animals, heart and lung weights were recorded and hearts were further dissected into the right ventricle (RV) and left ventricle plus septum (LV+S) and weighed. The RV/(LV+S) weight ratio was calculated as an indicator of right ventricular hypertrophy, characteristic of pulmonary hypertension. Additional lung tissue from control *Hmox1*^{+/+} C57BL/6J mice was also prepared without storage and shipment. No difference was noted between data obtained from tissue prepared directly or after storage. The number of sections and animals used are indicated in the relevant figure legend.

Western blotting: HO-1 and HO-2

Western blotting was performed to determine the level of HO-1 and HO-2 protein in porcine and murine whole lung tissue and porcine airway and intrapulmonary artery. The artery used for blotting was treated in exactly the same way as used for the organ bath experiments. Specifically, we can confirm that the vessels we used had no macrophages present since the tissue was dissected and cleared of adventitia and connective tissue (where macrophages may have been loosely associated with the vessel) and the lumen washed before tissue was prepared for blotting. Tissue was homogenised in Munroe Lysis buffer and centrifuged at 10,000 × g, for 10 min, at 4°C. The supernatants were removed from samples and snap frozen for storage. The protein content of the supernatants was determined by the Lowry procedure (Sigma protein assay kit, Sigma-Aldrich Company Ltd, Poole, Dorset, U.K.). Samples were mixed 1:1 with gel-loading buffer and separated by

SDS-PAGE performed on a 12% gel. Each well was loaded with 50 µg of sample protein (quantified in homogenate spectrophotometrically; equal protein loading was assessed qualitatively *via* Ponceau Red) or 1 ng of HO-1 or HO-2 protein standard (Stressgen Biotechnologies, Victoria, Canada). Each gel also contained a molecular mass rainbow marker (RMN756, Amersham Pharmacia Biotech U.K. Ltd, Buckinghamshire, U.K.). The separated blots were transferred by electrophoresis onto nitrocellulose membrane, blocked overnight (phosphate buffered saline (PBS)-tween, 5% milk) at 4°C, before incubation for 1 h at room temperature with polyclonal antibody directed against HO-1 or HO-2 (Stressgen Biotechnologies, Victoria, Canada) prepared in PBS at concentrations of 1:1000 and 1:2000, respectively. Membranes were then washed with PBS-tween and incubated for an hour with polyclonal goat anti-rabbit IgG antibodies conjugated with horseradish peroxidase (HRP) (1:2000, Sigma-Aldrich Company Ltd, Poole, Dorset, U.K.). After further washings, blots were incubated with a commercially available extended duration chemiluminescence substrate (Biowest™, UVP, Cambridge, U.K.) and bands visualised, captured and analysed utilising a GDS 8000 system attached to an Epi Chemi II darkroom.

Vasoreactivity

Conduit intrapulmonary arteries, dissected out from the lower lobes of 14-day-old piglets, were cleaned of connective tissue, cut into rings (1–2 mm in length, 1–2 mm in diameter) and mounted in 5 ml organ chambers containing gassed (95% O₂:5% CO₂), warmed (37°C), Krebs–Henseleit solution. Over 1-h equilibration period, a baseline tension of 1 g was applied (Arrigoni *et al.*, 1999). Rings were then maximally contracted with KCl (125 mM; approximately 5.5 mN; see Arrigoni *et al.*, 1999). After washing, each ring preparation, acting as its own control, was contracted to approximately 75% of its maximum response to KCl with the thromboxane mimetic U46619 (1×10^{-8} – 1×10^{-7} M). Preparations were then incubated in the presence or absence of the nonselective NO synthase (NOS) inhibitor, *N* ω -nitro-L-arginine methyl ester (L-NAME, 1×10^{-4} M) or the combined HO-1/HO-2 inhibitors chromium mesoporphyrin (CrMP: 5×10^{-6} M, Appleton *et al.*, 1999) and tin protoporphyrin (SnPP: 1×10^{-5} M, Sammut *et al.*, 1998), which were used in concentrations selective for the HO-1 pathway over the NOS pathway. Experiments were also carried out in the presence of the SnPP/CrMP vehicle sodium hydroxide. After a 30-min equilibration period, cumulative concentration–response curves were constructed to acetylcholine (ACh; 1×10^{-9} – 3×10^{-4} M). At the end of all experiments, to ensure smooth muscle viability, rings were maximally relaxed (i.e. approximately 100% of induced tone) with the NO donor sodium nitroprusside (SNP: 1×10^{-5} M). U46619, ACh, SNP and L-NAME were purchased from Sigma-Aldrich Company Ltd, Poole, Dorset, U.K. CrMP and SnPP were from Affinity research Products Ltd, Exeter, U.K. It should be noted that the HO inhibitors used in this study are nonselective for discrimination between HO-1, HO-2 or HO-3.

Immunohistochemistry

Porcine and murine (*Hmox1*^{+/+} and *Hmox1*^{-/-}) lung tissue was sectioned (4 µm) and stained with antibodies, as above,

specific for HO-1 (Stressgen Biotechnologies, Victoria, Canada) and smooth muscle α -actin (Sigma-Aldrich Company Ltd, Poole, Dorset, U.K.) respectively, using the streptavidin–biotin–peroxidase complex method. Sections were placed on a hot block (56°C) for 30 min, dewaxed in histoclear, and rehydrated in graded ethanol. Endogenous peroxidase was blocked by incubation in freshly prepared 0.3% hydrogen peroxide. Antigens were unmasked by autoclaving at 121°C for 14 min in citric acid buffer (pH adjusted to 6.0). Before incubation with primary antibody, sections were blocked with serum-free protein block (Dako Ltd, Cambridge, U.K.). Sections were then incubated for 1 h room temperature with anti HO-1 (1:500) or anti-smooth muscle α -actin (1:3000) diluted in PBS. After washing in PBS, sections were incubated for a further hour with goat anti-rabbit IgG (1:100 in PBS, Dako Ltd, Cambridge, U.K.). After further PBS washing, the sections were incubated with streptavidin-biotinylated HRP complex (1:200 dilution in PBS; Amersham Pharmacia Biotech U.K. Ltd, Buckinghamshire, U.K.) for 30 min at room temperature. The colour was developed using 3',3'-diaminobenzidine (Sigma-Aldrich Company Ltd, Poole, Dorset, U.K.). In control sections, incubation with primary antibody was omitted. Sections were counterstained with haematoxylin before visualisation under a light microscope (Leitz Dialux 20).

Image analysis

For *Hmox1*^{+/+} and *Hmox1*^{-/-} murine lung sections stained for smooth muscle α -actin, images were captured using a Zeiss AxioCam and analysed using Openlab software (v3.04, Improvision, Coventry, U.K.). The external diameter and area, and the lumen diameter and area, of muscular and partially muscular pulmonary arteries were measured. Medial wall thickness and area were calculated as a percentage of external diameter/area, respectively. Percentage of arteries muscular *versus* partially muscular in appearance was also calculated. A range of vessel sizes (20–100 µm in diameter) were analysed from each lung section studied.

Reverse transcription (RT)–polymerase chain reaction (PCR) and real-time PCR

Total RNA was isolated from snap-frozen lungs from mice by using the RNeasy Mini Kit (Qiagen) according to the manufacturer's instructions. cDNA was generated by RT using random hexamers. The cDNA (42 ng per reaction) was used as a template in the subsequent PCR analyses. Transcript levels were determined by real-time PCR (Rotor Gene 3000, Corbett Research, Australia) using the Syber Green PCR Master Mix Reagent Kit (Promega). The sequences for the mouse HO-1 PCR primer were sense 5'-GCCACCAAGGA GGTACACAT-3' and antisense 5'-GCTTGTTGCGCTCTAT CTCC-3' (Duckers *et al.*, 2001). Primers for mouse GAPDH were sense 5'-AACGACCCCTTCATTGAC-3' and antisense 5'-TCCACGACATACTCAGCAC-3'. Primers were used at a concentration of 0.5 µM for real-time PCR in each reaction. Cycling conditions for real-time PCR were as follows: step 1, 15 min at 95°C; step 2, 15 s at 94°C; step 3, 25 s at 60°C; step 4, 22 s at 72°C, with repeat from step 2 to step 4 for 40 times. Data from the reaction were collected and analysed by the complementary computer software (Corbett Research,

Australia). Relative quantitations of gene expression were calculated using standard curves and normalised to GAPDH.

Data analysis

All data are given as mean \pm s.e.m. Statistical tests used and the numbers of assays (*n*) are stated in the appropriate sections of text and figure legends.

Results

HO protein levels in porcine whole lung homogenate from foetal, NB, 1-, 3-, 14-day-old and adult pigs

HO-1 protein was low or undetectable in lungs from foetal animals, but increased after birth. In lungs from foetal, NB, 1-, 3- and 14-day-old pigs, HO-1 appeared as a single protein band consistent with a predicted molecular weight of 32 kDa. However, in lungs from adult pigs, HO-1 appeared as two separate bands, one of approximately 32 kDa and the other being smaller (Figure 1a and c). By contrast, the amount of HO-2 expressed was comparable in lungs from all age groups tested, with the exception of adult pigs, where levels were lower (Figure 1b and d).

Localisation of HO-1 in the porcine lung

In line with data obtained using Western blot analysis, immunohistochemical staining of porcine lung sections with an antibody specific for HO-1 showed low levels of staining in foetal sections (Figure 2a), increasing postnatally with age. HO-1 expression was greatest in sections taken from 14-day-old animals (Figure 2b). HO-1 was detected in all the

principal pulmonary structures including airway epithelium, bronchial smooth muscle, bronchial arteries, large pulmonary arteries and veins (data not shown). However, it was the

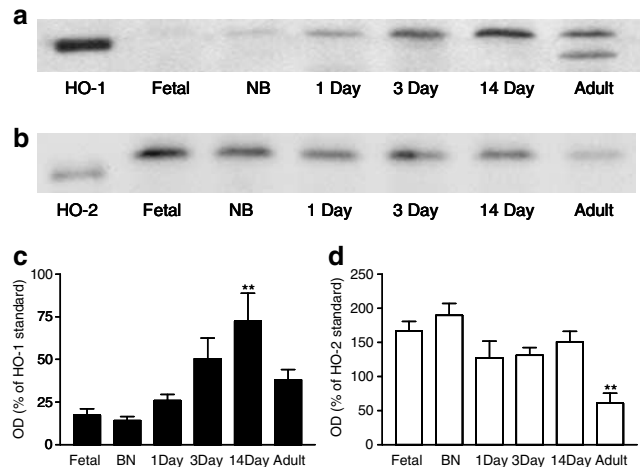


Figure 1 HO protein levels in porcine lungs from foetal, NB, 1-, 3-, 14-day-old and adult pigs. Representative Western blot of (a) HO-1 and (b) HO-2 protein expression in whole lung tissue harvested from foetal, NB, 1-, 3-, 14-day-old and adult pigs. Samples were separated by SDS-PAGE performed on a 12% gel. Each well was loaded with 50 μ g of sample protein (determined using the Lowry procedure) or 1 ng of HO-1/HO-2 standard. Blots, transferred by electrophoresis onto nitrocellulose membrane, were incubated with antibody directed against HO-1 or HO-2 (1 : 1000 and 1 : 2000, respectively). Pooled data are also shown for (c) HO-1 and (d) HO-2 protein levels (*n* = 6 separate Western blot experiments using separately prepared tissue extract from the lungs of *n* = 3 animals). Data (mean \pm s.e.m.) are expressed as a % of HO-1 or HO-2 standard (1 ng per well) calculated by measuring the optical density (OD) of the respective bands at 32 kDa. Only data from the top, the 32 kDa, band was included in (c). One-way ANOVA *versus* foetal: ***P* < 0.01.

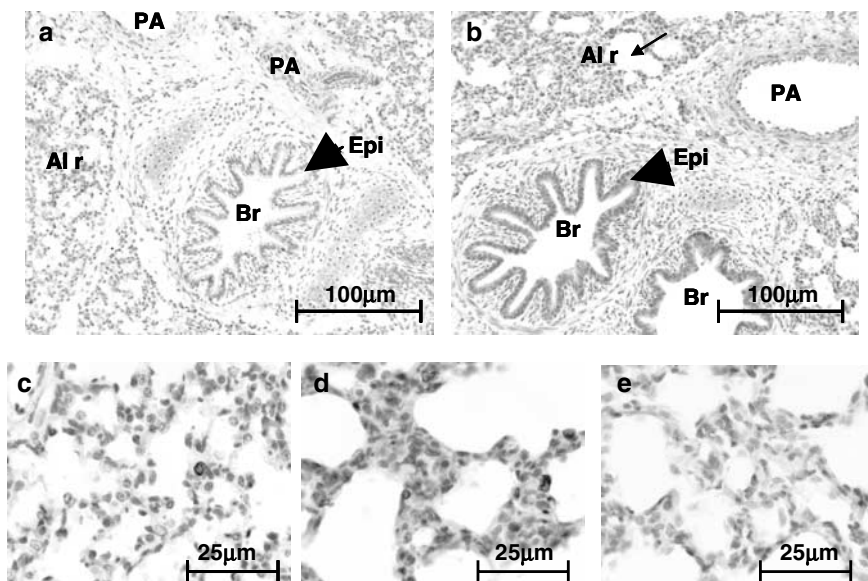


Figure 2 Localisation of HO-1 in the porcine lung. Porcine lung tissue was fixed in 10% formal saline, embedded in paraffin wax, sectioned (4 μ m) and stained with an antibody specific for HO-1 (dilution 1 : 500) using the streptavidin-biotin-peroxidase complex method. Figure showing HO-1 expression in (a) foetal and (b) 14-day-old porcine lung. In photographs of the same lung sections, at a higher magnification, panels (c) and (d) show the alveolar region of the foetal and 14-day-old animals, respectively. Panel (e) shows the negative control (no primary antibody) using tissue from the same 14-day-old animal. PA, pulmonary artery; Br, bronchus; Epi, epithelium; Al r, alveolar region. Slides are representative of sections studied from the three other animals in each age group.

presence of intense immunoreactive staining in alveolar macrophage-like cells that accounted for the majority of HO-1 in lungs from 14-day-old pigs (Figure 2d). However, these cells were sparsely present in foetal lung sections (Figure 2c).

The presence of HO-1 (and HO-2) in isolated pulmonary arteries and isolated airways dissected from the lungs of foetal and 14-day-old animals was confirmed by Western blotting. HO-1 was undetectable in vessels and airways from foetal animals, but was clearly present by 14 days of age (Figure 3a). HO-2 levels were not significantly different in foetal *versus* 14-day-old piglets (Figure 3b).

Role of HO activity in vasomotor responses of intrapulmonary artery rings from 14-day-old pigs; the peak of HO-1 expression

ACh induced a concentration-dependent vasodilator response of pulmonary arteries from 14-day-old pigs, an effect that was

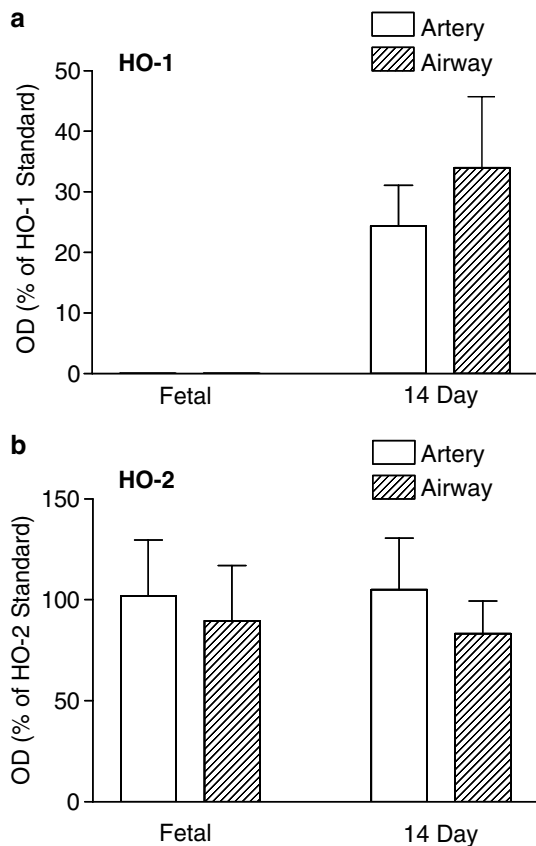


Figure 3 HO protein levels in porcine intrapulmonary artery and airway from foetal and 14-day-old animals. Intrapulmonary arteries and airways were dissected from the lower lobe of foetal and 14-day-old piglet lungs. Samples were separated by SDS-PAGE performed on a 12% gel. Each well was loaded with 50 μ g of sample protein (determined using the Lowry procedure) or 1 ng of HO-1/HO-2 standard. Blots, transferred by electrophoresis onto nitrocellulose membrane, were incubated with antibody directed against HO-1 or HO-2 (1:1000 and 1:2000, respectively). Figure shows the protein expression of (a) HO-1 and (b) HO-2 protein in intrapulmonary artery ($n=4$ animals for both age groups) and airway ($n=4$ animals for both age groups) from foetal and 14-day-old piglet lungs. Data (mean \pm s.e.m.) are expressed as a % of HO-1 or HO-2 standard (1 ng per well) calculated by measuring the OD of the respective bands at 32 kDa. One-way ANOVA *versus* foetal: * $P<0.05$.

completely blocked by the NOS inhibitor L-NAME (1×10^{-4} M) but was not inhibited by two separate inhibitors of HO activity, SnPP and CrMP (1×10^{-5} and 5×10^{-6} M, respectively), (Figure 4). The SnPP and CrMP vehicle, NaOH, had no effect on the ACh-induced vasodilator response. When L-NAME was added to pre-constricted pulmonary arteries, a further constriction was noted, consistent with inhibition of 'basal' release of endothelial-derived NO. In parallel tissues, no such increase in tone was observed with either of the HO inhibitors or their vehicle. In contrast to L-NAME, CrMP actually reduced tone (vehicle *versus* CrMP: 105.4 ± 7.7 *versus* $59.4 \pm 10.4\%$ of U46619-induced tone, $P<0.001$, Mann-Whitney, $n=8$ rings from $n=4$ animals in both groups) (Figure 4b).

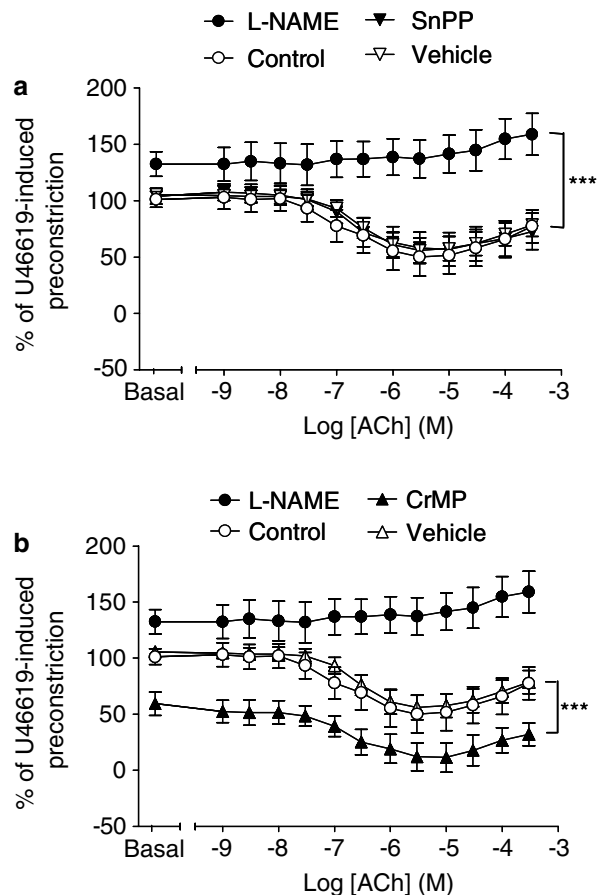


Figure 4 Role of HO activity in vasomotor responses of intrapulmonary artery rings from 14-day-old pigs; the peak of HO-1 expression. Intrapulmonary arteries were dissected from the lower lobe of lungs harvested from 14-day-old piglets. Ring preparations were mounted in 5 ml organ chambers containing gassed (95% O_2 :5% CO_2), warmed ($37^\circ C$), Krebs-Henseleit solution. Over a 1-h equilibration period, a baseline tension of 1 g was applied. Rings were precontracted with the thromboxane mimetic U46619 before 30 min incubation with L-NAME (1×10^{-4} M), SnPP (1×10^{-5} M), CrMP (5×10^{-6} M) or the NaOH vehicle. The effects of L-NAME, (a) SnPP and (b) CrMP on pre-constricted tone, and on dilator responses of ring preparations to ACh, were expressed as a % of U46619-induced tone (mean \pm s.e.m., $n=8$ from $n=4$ animals). L-NAME *versus* control: *** $P<0.0001$, two-way ANOVA. CrMP *versus* vehicle: *** $P<0.0001$, two-way ANOVA.

Characterisation of HO protein and gene expression in murine lungs at the after birth

Similar to observations made with porcine lungs, HO-1 protein expression increased in the lungs of mice after birth (Figure 5a and c). In addition, mRNA for HO-1 was also highest at the post-natal time points (1 and 3 days; Figure 6). Both protein and message levels were reduced in lung tissue at 14 days after birth. HO-2 was clearly detectable and remained unchanged, in the lungs of mice from all age groups (Figure 5b and d). In

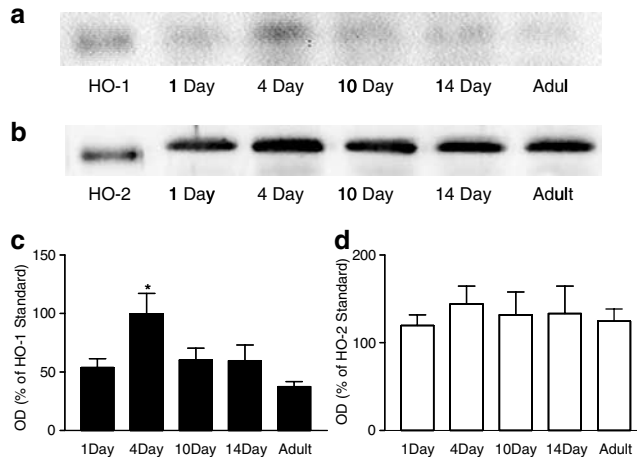


Figure 5 HO protein levels in murine lungs from 1-, 4-, 10-, 14-day-old and adult mice. Representative Western blot of (a) HO-1 and (b) HO-2 protein expression in whole lung tissue harvested from 1-, 4-, 10-, 14-day-old and adult C57BL/6J mice. Samples were separated by SDS-PAGE performed on a 12% gel. Each well was loaded with 50 μ g of sample protein (determined using the Lowry procedure) or 1 ng of HO-1/HO-2 standard. Blots, transferred by electrophoresis onto nitrocellulose membrane, were incubated with antibody directed against HO-1 or HO-2 (1:1000 and 1:2000, respectively). Pooled Western blot data are also shown for (c) HO-1 and (d) HO-2 ($n=4$ animals in all age groups). Data (mean \pm s.e.m.) are expressed as a % of HO-1 or HO-2 standard (1 ng per well) calculated by measuring the OD of the respective bands at 32 kDa. Only data from the top, the 32 kDa, band was included in (c). One-way ANOVA *versus* 1-day old: * $P<0.05$.

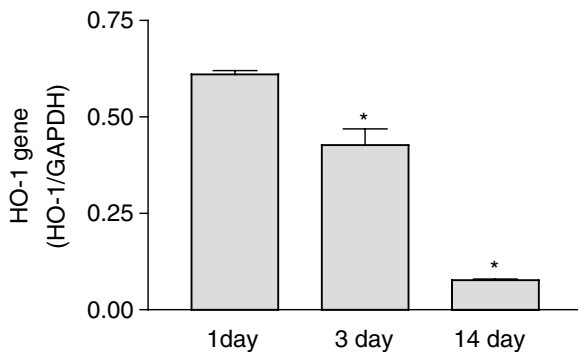


Figure 6 Levels of mRNA for HO-1 gene in the lungs of mice at 1, 3 or 14 days after birth. mRNA was measured by real-time PCR. Results are shown as a ratio of HO-1 to GAPDH. Results are the mean \pm s.e.m. of $n=6$ using lungs from two separate litters. Data were analysed using one-way ANOVA and a P -value of <0.05 denoted by *.

contrast to our observations in the pig lung, no double band of HO-1, or fall in HO-2 protein levels was observed in adult murine tissue.

Postnatal remodelling of the normal murine pulmonary vasculature

The rapid remodelling of the pulmonary vasculature after the transition from placental to air breathing has been well characterised in pigs, where a significant reduction in arterial wall thickness is observed during the first week of life (Haworth & Hislop, 1981). Here we report that a similar phenomenon occurs in the mouse lung. In lungs from our youngest mice (1-day-old), a high percentage of pulmonary vessels appeared 'immature'. Specifically, endothelial cells bulged into the lumen and the media was thick (not shown). By 3–5 days, the pulmonary arteries had a flattened endothelium and thinner walls, the pattern of change with age being similar to that described in other species (Haworth & Hislop, 1981; 1983; Meyrick & Reid, 1992). Pulmonary artery medial vessel wall thickness and medial area continued to diminish after 3–5 days (Figure 7). The percentage of muscular, as opposed to partially muscular, vessels increased with vessel diameter and decreased in each size range during the first 14 days of life and beyond that age in the smaller arteries (Figure 8).

Pulmonary vascular remodelling in HO-1-deficient mice

Disruption of the HO-1 gene was not associated with evidence of specific morphological characteristics for pulmonary hypertension in the adult mice. Thus, neither pulmonary artery medial wall thickness (Figure 9a), medial wall area (Figure 9b) nor RV/LV + S ratio ($Hmox1^{+/+}$ *versus* $Hmox1^{-/-}$: 0.26 ± 0.02

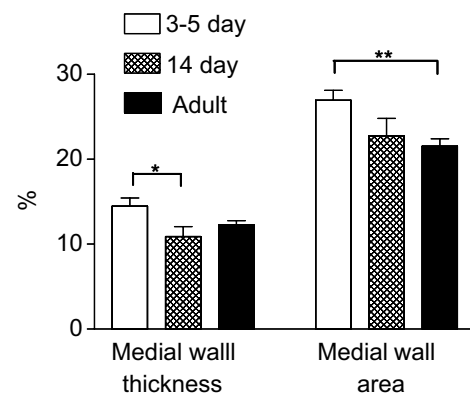


Figure 7 Postnatal remodelling of the normal murine pulmonary vasculature. Lung tissue from 3–5-day-old, 14-day-old and adult mice (C57BL/6J) was fixed in 10% formal saline, embedded in paraffin wax, sectioned (4 μ m) and stained using an antibody specific for smooth muscle α -actin (dilution 1:3000) using the streptavidin-biotin-peroxidase complex method. Images were captured using a Zeiss AxioCam and analysed using Openlab. The external and internal diameter, and area, of muscular and partially muscular pulmonary arteries was measured. Percentage medial wall thickness/area was then calculated. The figure shows percentage medial wall thickness/area from 3- and 5-day-old, 14-day-old and adult mice (≥ 150 vessels, 20–100 μ m in diameter, from $n=4$ –6 animals were analysed). Data are mean \pm s.e.m. Student's t -test: * $P<0.05$, ** $P<0.01$.

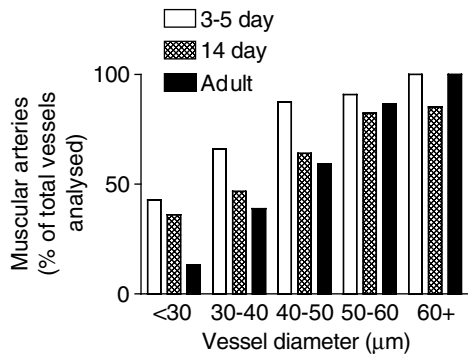


Figure 8 Percentage of muscular arteries in normal 3–5-day-old, 14-day-old and adult mice. Lung tissue from 3–5-day-old, 14-day-old and adult mice (C57BL/6J) was fixed in 10% formol saline, embedded in paraffin wax, sectioned (4 μm) and stained using an antibody specific for smooth muscle α -actin (dilution 1 : 3000) using the streptavidin–biotin–peroxidase complex method. Images were captured using a Zeiss AxioCam. The figure shows the number of muscular arteries analysed, as a percentage of total arterial vessels analysed, in each age group (11–52 vessels from $n=4$ –6 animals were analysed).

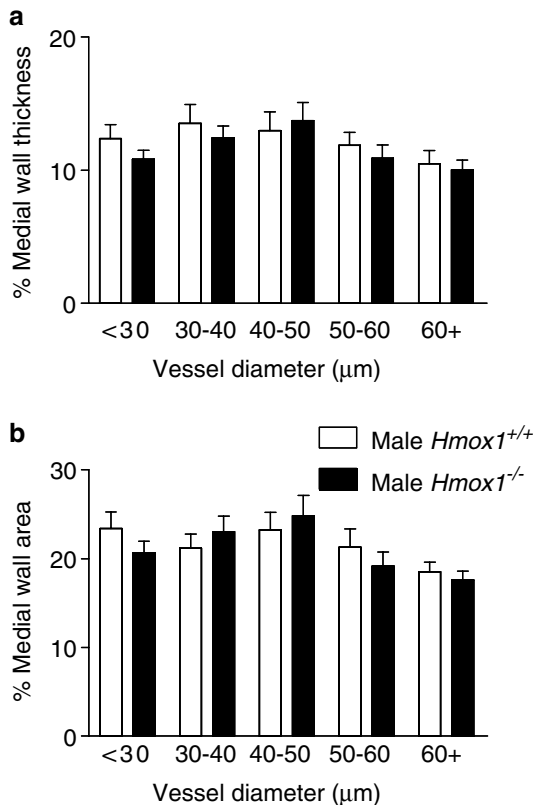


Figure 9 Pulmonary vascular structure in adult male HO-1 deficient mice. Murine adult male ($Hmox1^{+/+}$ and $Hmox1^{-/-}$) lungs were fixed in 10% formol saline, embedded in paraffin wax, sectioned (4 μm) and stained using an antibody specific for smooth muscle α -actin (dilution 1 : 3000) using the streptavidin–biotin–peroxidase complex method. Images were captured using a Zeiss AxioCam and analysed using Openlab. The external and internal diameter, and area, of muscular and partially muscular pulmonary arteries was measured. Percentage medial wall thickness/area was then calculated. (a) Percentage medial wall thickness and (b) percentage medial wall area of arteries from adult male $Hmox1^{+/+}$ (15–45 vessels from $n=6$ animals were analysed) and adult male $Hmox1^{-/-}$ (22–41 vessels from $n=6$ animals were analysed) mice. Data are mean \pm s.e.m. No significant difference (two-way ANOVA) was observed between the two groups.

versus 0.25 ± 0.01 , $n=6$) were significantly different in vessels from adult $Hmox1^{-/-}$ and $Hmox1^{+/+}$ mice. The percentage of muscular vessels, within each vessel diameter range, from adult $Hmox1^{-/-}$ versus $Hmox1^{+/+}$ mice was found to be comparable (data not shown). Also, no significant difference was observed in pulmonary vessel architecture between adult male $Hmox1^{-/-}$ versus adult female $Hmox1^{-/-}$ mice (Figure 10). Similar RV/LV+S ratio did not exhibit a gender difference (male versus female: 0.25 ± 0.01 versus 0.26 ± 0.02 , $n=6$ and 5 respectively).

In line with data obtained with adult mice, no differences were observed in the pulmonary vascular remodelling occurring in the NB period. Thus, medial wall thickness (data not shown) and medial wall area (Figure 11a) were not significantly different in 3–5-day-old $Hmox1^{+/+}$ versus $Hmox1^{-/-}$ animals. Similarly, medial wall thickness (data not shown) and medial wall area (Figure 11b) did not differ between 14-day-old $Hmox1^{+/+}$ and 14-day-old $Hmox1^{-/-}$ animals.

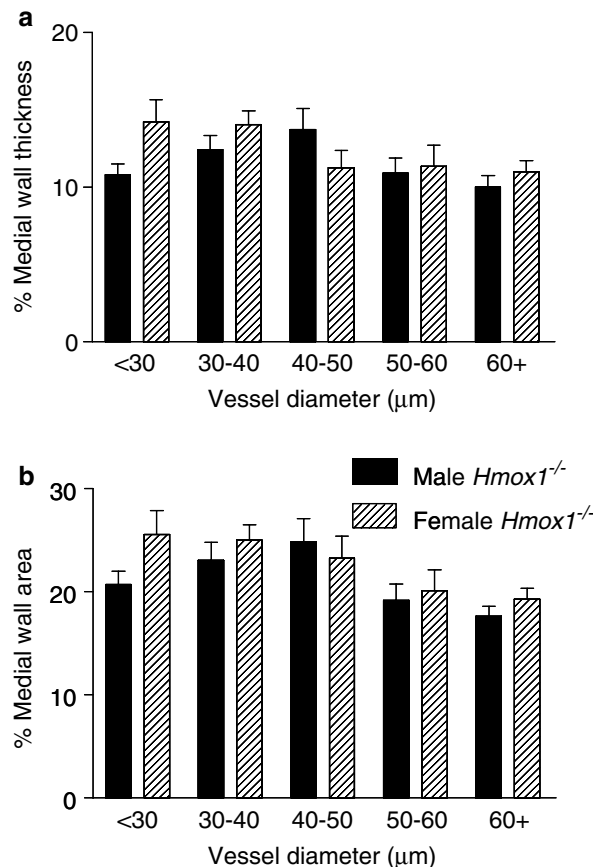


Figure 10 Pulmonary vascular structure in adult male versus adult female, HO-1 deficient mice. Lung tissue harvested from adult male $Hmox1^{-/-}$ mice and adult female $Hmox1^{-/-}$ mice was fixed in 10% formol saline, embedded in paraffin wax, sectioned (4 μm) and stained using an antibody specific for smooth muscle α -actin (dilution 1 : 3000) using the streptavidin–biotin–peroxidase complex method. Images were captured using a Zeiss AxioCam and analysed using Openlab. The external and internal diameter, and area, of muscular and partially muscular pulmonary arteries was measured. Percentage medial wall thickness/area was then calculated. (a) Percentage medial wall thickness and (b) percentage medial wall area of arteries from adult male $Hmox1^{-/-}$ (22–41 vessels from $n=6$ animals were analysed), and adult female $Hmox1^{-/-}$ (12–38 vessels from $n=5$ animals were analysed), mice. Data are mean \pm s.e.m. No significant difference (two-way ANOVA) was observed between the two groups.

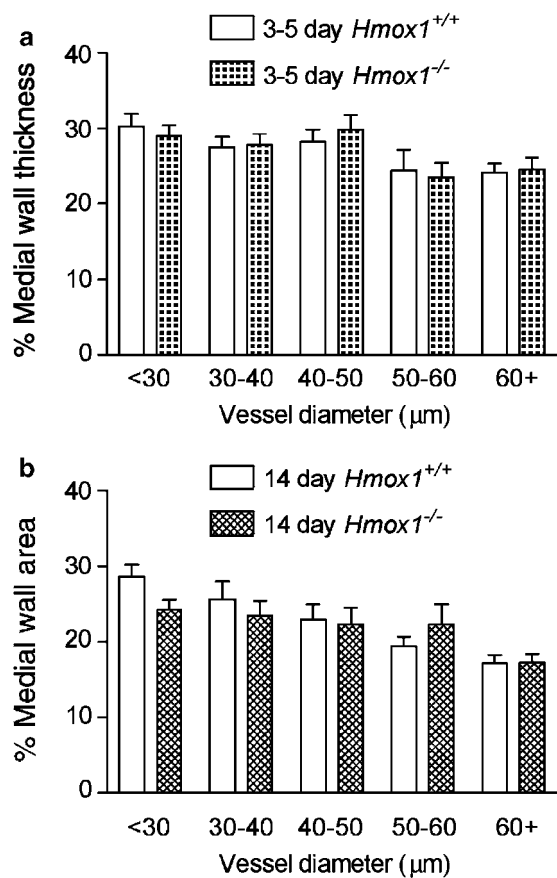


Figure 11 Postnatal remodelling of the pulmonary vasculature in HO-1 deficient mice. Lung tissue from 3–5-day-old and 14-day-old (*Hmox1*^{+/+} and *Hmox1*^{-/-}) mice was fixed in 10% formol saline, embedded in paraffin wax, sectioned (4 µm) and stained using an antibody specific for smooth muscle α -actin (dilution 1 : 3000) using the streptavidin–biotin–peroxidase complex method. Images were captured using a Zeiss AxioCam and analysed using Openlab. The external and internal areas of muscular and partially muscular pulmonary arteries were measured. Percentage medial wall area was then calculated. The figure shows the percentage medial wall thickness from (a) 3–5-day-old *Hmox1*^{+/+} (11–52 vessels from $n=4$ animals were analysed) and *Hmox1*^{-/-} (14–52 vessels from $n=6$ animals were analysed) mice and (b) 14-day-old *Hmox1*^{+/+} (17–52 vessels from $n=4$ animals were analysed) and *Hmox1*^{-/-} (14–43 vessels from $n=3$ animals were analysed) mice. Data are mean \pm s.e.m. No significant difference (two-way ANOVA) was observed between the *Hmox1*^{+/+} and *Hmox1*^{-/-} mice in either age group.

The percentage of muscular vessels, within each vessel diameter range, from *Hmox1*^{+/+} and *Hmox1*^{-/-} mice of the same age group were found to be comparable (data not shown).

Discussion

At birth, the lung undergoes dramatic functional, structural and secretory changes associated with the transition from placental to air breathing. These adaptive processes are not fully understood, but when they fail persistent pulmonary hypertension of the NB may occur. Here we show, for the first time, that HO-1 is temporally induced in a number of key pulmonary structures, including blood vessels immediately following birth. We also show, however, that HO-1 presence in

these structures does not appear to influence the critical adaptive changes in vasomotor or remodelling responses.

We found that lung samples from foetal, neonatal or adult pigs contained detectable levels of the constitutive form of HO, HO-2. HO-2 was manifest as a single protein band on Western blots that migrated at approximately 36 kDa molecular weight. Levels of HO-2 in lung tissue did not vary between any of the neonatal age groups (up to 14 days) studied. By contrast, HO-1 protein levels displayed a dramatic increase after birth, which continued for up to 14 days after birth. Again, as expected, HO-1 migrated as a single protein band at approximately 32 kDa molecular weight. For both HO-1 and HO-2, there was an apparent decline in protein levels in lungs from adult pigs compared to the 14-day-old animals. In the case of HO-1, the levels present in adult lungs were still clearly higher than those present in foetal or NB lungs. However, in lungs from adult pigs, HO-1 immunoreactivity appeared in two bands, which when combined would produce levels equivalent to those seen in the 14-day age groups. Through necessity, lung tissue from adult pigs was collected from abattoirs and, unlike lungs from the neonatal pigs, was not obtained and prepared freshly in the laboratory. Since in our experiments there was potential for protein degradation, it is not possible to comment on the relevance of the drop in HO levels in adult lung tissue. In line with our observations, the induction of HO-1 during lung maturation has recently been reported in rat whole lung tissue (Dennery *et al.*, 2003).

The low or undetectable levels of HO-1 in foetal lungs shown by Western blotting were confirmed using immunohistochemistry, showing no defined staining in any pulmonary structures at this time. However, HO-1 was detected in abundance in the lungs of 14-day-old pigs and was localised to blood vessels, airways and macrophage-like immune cells present within the alveolar space. Using Western blot analysis of isolated structures, the dramatic increase in HO-1 in vessels and airways was confirmed.

Induction of the HO/CO pathway is increasingly recognised as important in the regulation of vasomotor responses (Sammur *et al.*, 1998). CO relaxes blood vessels directly via the activation of SGC (Morita *et al.*, 1995). Inhibitors of HO, such as SnPP, inhibit endothelium-dependent vasodilatation (Zakhary *et al.*, 1996). We have shown previously that pulmonary vessels from foetal pigs do not possess a mature, fully developed endothelium-dependent vasodilator function (Liu *et al.*, 1992; Tulloh *et al.*, 1997; Arrigoni *et al.*, 1999); by 14 days after birth, pulmonary vessels possess a fully functional endothelium and dilate when stimulated appropriately. In the present study, we found that despite clear postnatal induction of HO-1, greatest in the vessels of 14-day-old animals, no evidence could be found of any contribution of HO activity to vasomotor responses at this age. Firstly, the endothelium-dependent dilator responses induced by ACh were not inhibited by two chemically different inhibitors of HO (Appleton *et al.*, 1999), while, as expected, the NOS inhibitor L-NAME completely inhibited ACh-induced relaxation. L-NAME has been used as a tool to decipher the role of NO in vascular responses for more than 10 years. The overwhelming numbers of publications attribute its effect to the specific inhibition of NOS activity. Nevertheless, it should be noted that a small number of studies have suggested that L-NAME has antimuscarinic effects independently of the NOS pathway (Buxton *et al.*, 1993). In the case of the current study,

we believe that the effects of L-NAME are specific to NOS inhibition, since its effects in large vessels are reversible by pretreatment with L-arginine. Secondly, when applied directly to precontracted blood vessels, neither of the HO inhibitors increased basal tone although L-NAME did do so, thus confirming the functional relevance of basally released NO in these tissues. The HO inhibitor CrMP actually induced vasodilatation. The explanation for this observation remains to be elucidated. One possibility is that, under basal conditions, the HO/CO pathway exerts inhibitory effects on the NOS pathway. This phenomenon has been demonstrated in smooth muscle strips from the rabbit internal anal sphincter where Chakder *et al.* (1996) observed that inhibitors of NOS reverse the fall in basal tone due to a third HO inhibitor, zinc protoporphyrin. Alternatively, CrMP may directly or indirectly activate vasodilatation by a mechanism unrelated to its actions on HO.

Based on the results of our organ bath experiments, upregulation of HO-1 in the porcine lung appears unlikely to play a role in the regulation of vascular tone after birth. However, the HO/CO pathway also has antiproliferative and antiapoptotic actions in systemic vascular tissue (Peyton *et al.*, 2002). The remodelling that occurs after vascular injury *in vivo* is increased significantly when the HO-1 gene has been deleted (Duckers *et al.*, 2001). In the pulmonary vasculature, we have recently shown that CO inhibits proliferation of adult human pulmonary vascular smooth muscle cells in culture (Stanford *et al.*, 2003). Others have found that, in transgenic mice where HO-1 is overexpressed, pulmonary vascular remodelling is reduced in response to chronic hypoxia (Minamino *et al.*, 2001). Perhaps therefore, HO-1 induction at birth may mediate the vascular remodelling that constitutes adaptation to extra-uterine life. This point can be addressed using mice where the gene encoding HO-1 (*Hmox1*^{-/-}) has been deleted (Duckers *et al.*, 2001).

In the current study, we found no evidence of the pulmonary hypertensive phenotype in adult male *Hmox1*^{-/-} mice, as assessed by RV/LV + S (an indication of right ventricular hypertrophy) or by vessel medial wall thickness/area. Previously, Yet *et al.* (1999) had noted no difference in the ventricular weights of adult *Hmox1*^{-/-} versus adult control mice. To rule out the possibility that targeted disruption of a gene may result in gender differences (Hislop *et al.*, 2003), we compared adult male and adult female *Hmox1*^{-/-} mice. No difference was observed between either the RV/LV + S weight ratio or vessel wall thickness/area in adult male *Hmox1*^{-/-} mice versus adult female *Hmox1*^{-/-} mice. Although we found no evidence of pulmonary hypertension in adult *Hmox1*^{-/-} mice, we studied the neonatal lungs to see if there was any evidence of a tendency to develop PPHN.

Similar to the data obtained with the porcine tissue, we found that HO-1 protein was induced in mice lungs after birth. HO-1 protein was low in the first 24 h after birth and increased at the 4-day time point. Protein levels were reduced by 14 days after birth. In addition, we measured mRNA levels in murine lungs from newborn (within 24 h of birth) 4- and 14- day age groups. The data we obtained were partly in line with our Western blot data. Levels of HO-1 gene were highest at 1 and 4 days after birth and had reduced by 80–90% by the 14-day time point. It was not technically possible for us to obtain lung material from foetal mice and so we cannot conclude that the high levels in the newborn period are higher than those in the foetal, or if the induction is coincident with breathing

(as we were able to do in the pig). However, with the sharp decline at 14 days and with the knowledge that message always precedes protein, this seems the most likely explanation.

As in the pig, HO-2 was detected in the lung tissue at all ages and levels did not vary greatly. The normal process of pulmonary vascular remodelling at birth has been well characterised in the porcine (Haworth & Hislop, 1981), human (Haworth & Hislop, 1983), ovine (Abman *et al.*, 1989) and rat (Meyrick & Reid, 1982) lung, where rapid remodelling of arterial wall thickness begins within 30 min and continues throughout the first 2 weeks of life. However, the nature of pulmonary vascular remodelling in this period has not previously been well documented in the mouse. We found that, in mice lungs, extensive remodelling had already occurred by 3–5 days after birth. Vessel wall thickness and area continued to decline into adulthood.

Despite the clear evidence that both HO-1 protein and mRNA were the highest in the lung during the period of post partum vascular adaptation, we found no evidence to suggest that its activity modulated vascular remodelling. Specifically, we found no difference in vessel wall thickness/area of 3–5-day-old *Hmox1*^{-/-} mice compared with control animals. Similarly, no difference was observed between 14-day-old *Hmox1*^{-/-} mice versus age-matched controls.

A recent study reports that HO-1 mRNA expression is decreased in the lungs of NB babies with congenital diaphragmatic hernia complicated by PPHN (Solari *et al.*, 2003). Indeed, the authors of the study suggest that the down-regulation of HO-1 mRNA, and thus endogenous CO production, may contribute to the altered vascular tone and underlie the vascular smooth muscle cell proliferation associated with PPHN. Our study would indicate that this is not in fact the case in the mice where a total lack of HO-1 has no impact on pulmonary vascular remodelling.

In conclusion, HO-1 but not HO-2 is upregulated in the lung at birth. Induction of HO-1 in the pulmonary arteries does not appear to play a major role in the regulation of vascular tone in the neonatal period. Adult mice lacking the gene encoding HO-1 do not appear to have pulmonary hypertension, nor does the absence of this gene affect the normal process of postnatal structural remodelling. There are a number of potential explanations for these observations. Firstly, HO-2 might compensate for the absence of HO-1 activity in *Hmox1*^{-/-} mice. However, this explanation would only apply to our remodelling data and would not account for the lack of involvement of HO activity (HO-1 plus HO-2) in the modulation of vasomotor tone in pulmonary blood vessels. Furthermore, HO-2 does not compensate for HO-1, in the same mice as we have used, in a model of carotid injury and subsequent arteriosclerosis (Duckers *et al.*, 2001). Secondly, high levels of HO-1 in the lung at birth may represent a redundant response to oxidative stress in the healthy sterile environment of a laboratory. If this were the case, we may see very different effects if our animals were exposed to an additional stress at birth. Indeed, in humans, inhalation of meconium is one clinical event which can result in PPHN. It is tempting to speculate therefore that HO-1 in the lungs at birth is an evolutionary prophylactic response to the increased risk of infection, inflammation or aspiration. Finally, HO-1 induction in the lung at birth may have functional consequences in structures other than the blood vessels, such as in the airway or immune cells, both of which were enriched sites of expression.

References

- ABMAN, S.H., SHANLEY, P.F. & ACCURSO, F.J. (1989). Failure of postnatal adaptation of the pulmonary circulation after chronic intrauterine pulmonary hypertension in foetal lambs. *J. Clin. Invest.*, **83**, 1849–1858.
- APPLETON, S.D., CHRETIEN, M.L., MCLAUGHLIN, B.E., VREMAN, H.J., STEVENSON, D.K., BRIEN, J.F., NAKATSU, K., MAURICE, D.H. & MARKS, G.S. (1999). Selective inhibition of heme oxygenase, without inhibition of nitric oxide synthase or soluble guanylyl cyclase, by metalloporphyrins at low concentrations. *Drug Metab. Dispos.*, **27**, 1214–1219.
- ARRIGONI, F.I., HISLOP, A.A., HAWORTH, S.G. & MITCHELL, J.A. (1999). Newborn intrapulmonary veins are more reactive than arteries in normal and hypertensive piglets. *Am. J. Physiol.*, **277** (Part 1), L887–L892.
- BAK, I., SZENDREI, L., TUROCZI, T., PAPP, G., JOO, F., DAS, D.K., DE LEIRIS, J., DER, P., JUHASZ, B., VARGA, E., BACSKAY, I., BALLA, J., KOVACS, P. & TOSAKI, A. (2003). Heme oxygenase-1-related carbon monoxide production and ventricular fibrillation in isolated ischemic/reperfused mouse myocardium. *FASEB J.*, **17**, 2133–2135.
- BRAGGINS, P.E., TRAKSHEL, G.M., KUTTY, R.K. & MAINES, M.D. (1986). Characterisation of two heme oxygenase isoforms in rat spleen: comparison with the hematin-induced and constitutive isoforms of the liver. *Biochem. Biophys. Res. Commun.*, **141**, 528–533.
- BUXTON, I.L., CHEEK, D.J., ECKMAN, D., WESTFALL, D.P., SANDERS, K.M. & KEEF, K.D. (1993). NG-nitro L-arginine methyl ester and other alkyl esters of arginine are muscarinic receptor antagonists. *Circ. Res.*, **72**, 387–395.
- CARRAWAY, M.S., GHIO, A.J., SULIMAN, H.B., CARTER, J.D., WHORTON, A.R. & PIANTADOSI, C.A. (2002). Carbon monoxide promotes hypoxic vascular remodelling. *Am. J. Physiol. Lung. Cell Mol. Physiol.*, **282**, L693–L702.
- CHAKDER, S., RATHI, S., MA, X.L. & RATTAN, S. (1996). Heme oxygenase inhibitor zinc protoporphyrin IX causes an activation of nitric oxide synthase in the rabbit internal anal sphincter. *J. Pharmacol. Exp. Ther.*, **277**, 1376–1382.
- DENNERY, P.A., LEE, C.S., FORD, B.S., WENG, Y.H., YANG, G. & RODGERS, P.A. (2003). Developmental expression of heme oxygenase in the rat lung. *Pediatr. Res.*, **53**, 42–47.
- DUCKERS, H.J., BOEHM, M., TRUEM, A.L., YETM, S.-F., SAN, H., PARK, J.L., WEBB, R.C., LEE, M.-E., NABEL, G.J. & NABEL, E.G. (2001). Heme oxygenase-1 protects against vascular constriction and proliferation. *Nature Med.*, **7**, 693–698.
- DURANTE, W. (2002). Carbon monoxide and bile pigments: surprising mediators of vascular function. *Vasc. Med.*, **7**, 195–202.
- EWING, J.F. & MAINES, M.D. (1995). Distribution of constitutive (HO-2) and heat-inducible (HO-1) heme oxygenase isoenzymes in the rat testes: HO-2 displays stage-specific expression in germ cells. *Endocrinology*, **136**, 2294–2302.
- HAWORTH, S.G. & HISLOP, A.A. (1981). Adaptation of the pulmonary circulation to extra-uterine life in the pig and its relevance to the human infant. *Cardiovasc. Res.*, **15**, 108–119.
- HAWORTH, S.G. & HISLOP, A.A. (1983). Pulmonary vascular development: normal values of peripheral vascular structure. *Am. J. Cardiol.*, **52**, 578–583.
- HAYASHI, S., TAKAMIYA, R., YAMAGUCHI, T., MATSUMOTO, K., TOJO, S.J., TAMATANI, T., KITAJIMA, M., MAKINO, N., ISCIMURA, Y. & SUEMATSU, M. (1999). Induction of heme oxygenase-1 suppresses venular leukocyte adhesion elicited by oxidative stress: role of bilirubin generated by the enzyme. *Circ. Res.*, **85**, 663–671.
- HISLOP, A.A., MILLER, A.A., STIDWELL, R., VALLANCE, P. & HAWORTH, S.G. (2003). Postnatal adaptation of pulmonary arteries is gender dependent in endothelial nitric oxide synthase deficient mice. *Am. J. Resp. Crit. Care Med.*, **167**, A3104.
- LIU, S.F., HISLOP, A.A., HAWORTH, S.G. & BARNES, P.J. (1992). Developmental changes in endothelium-dependent pulmonary vasodilatation in pigs. *Br. J. Pharmacol.*, **106**, 324–330.
- MCCOUBREY Jr, W.K., HUANG, T.J. & MAINES, M.D. (1997). Isolation and characterization of a cDNA from the rat brain that encodes hemoprotein heme oxygenase-3. *Eur. J. Biochem.*, **247**, 725–732.
- MEYRICK, B. & REID, L. (1982). Pulmonary arterial and alveolar development in normal postnatal rat lung. *Am. Rev. Respir. Dis.*, **125**, 468–473.
- MINAMINO, T., CHRISTOU, H., HSIEH, C.M., LIU, Y., DHAWAN, V., ABRAHAM, N.G., PERRELLA, M.A., MITSIALIS, S.A. & KOUREMBANAS, S. (2001). Targeted expression of heme oxygenase-1 prevents the pulmonary inflammatory and vascular responses to hypoxia. *Proc. Natl. Acad. Sci. U.S.A.*, **98**, 8798–8803.
- MORITA, T., PERRELLA, M.A., LEE, M.E. & KOUREMBANAS, S. (1995). Smooth muscle cell-derived carbon monoxide is a regulator of vascular cGMP. *Proc. Natl. Acad. Sci. U.S.A.*, **92**, 1475–1499.
- MOTTERLINI, R., CLARK, J.E., FORESTI, R., SARATHCHANDRA, P., MANN, B.E. & GREEN, C.J. (2002). Carbon monoxide-releasing molecules: characterisation of biochemical and vascular activities. *Circ. Res.*, **90**, E17–E24.
- PEYTON, K.J., REYNA, S.V., CHAPMAN, G.B., ENSENAT, D., LIU, X.M., WANG, H., SCHAFER, A.I. & DURANTE, W. (2002). Heme oxygenase-1-derived carbon monoxide is an autocrine inhibitor of vascular smooth muscle cell growth. *Blood*, **99**, 4443–4448.
- SAMMUT, I.A., FORESTI, R., CLARK, J.E., EXON, D.J., VESELY, M.J., SARATHCHANDRA, P., Green, C.J. & Motterlini, R. (1998). Carbon monoxide is a major contributor to the regulation of vascular tone in aortas expressing high levels of heme oxygenase-1. *Br. J. Pharmacol.*, **25**, 1437–1444.
- SOLARI, V., PIOTROWSKA, A.P. & PURI, P. (2003). Expression of heme oxygenase-1 and endothelial nitric oxide synthase in the lung of newborns with congenital diaphragmatic hernia and persistent pulmonary hypertension. *J. Pediatr. Surg.*, **38**, 808–813.
- STANFORD, S.J., WALTERS, M.J., HISLOP, A.A., HAWORTH, S.G., EVANS, T.W. & MITCHELL, J.A. (2003). Heme oxygenase is expressed in human pulmonary artery smooth muscle where carbon monoxide has an anti-proliferative role. *Eur. J. Pharmacol.*, **25**, 135–141.
- TULLOH, R.M., HISLOP, A.A., BOELS, P.J., DEUTSCH, J. & HAWORTH, S.G. (1997). Chronic hypoxia inhibits postnatal maturation of porcine intrapulmonary artery relaxation. *Am. J. Physiol.*, **272**, H2436–H2445.
- YET, S.F., PERRELLA, M.A., LAYNE, M.D., HSIEH, C.M., MAEMURA, K., KOBZIK, L., WIESEL, P., CHRISTOU, H., KOUREMBANAS, S. & LEE, M.E. (1999). Hypoxia induces severe right ventricular dilatation and infarction in heme oxygenase-1 null mice. *J. Clin. Invest.*, **108**, R23–R29.
- ZAKHARY, R., GAINE, S.P., DINERMAN, J.L., RUAT, M., FLAVAHAN, N.A. & SNYDER, S.H. (1996). Heme oxygenase 2: endothelial and neuronal localization and role in endothelium-dependent relaxation. *Proc. Natl. Acad. Sci. U.S.A.*, **93**, 795–798.

(Received February 12, 2004

Revised May 7, 2004

Accepted August 26, 2004)